PNAS
www.pnas.org

Supplementary Information for

Lysosomal degradation products induce *Coxiella burnetii* virulence

Patrice Newton, David R Thomas, Shawna CO Reed, Bangyan Xu, Nicole Lau, Sze Ying Ong, Shivani Pasricha, Piyush B Madhamshettiwar, Laura E Edgington-Mitchell, Kaylene J Simpson, Craig R Roy and Hayley J Newton

Corresponding Author: Hayley J Newton
Email: hnewton@unimelb.edu.au

This PDF file includes:

SI Materials and Methods
Figs. S1 to S3
Tables S1 to S4

Other supplementary materials for this manuscript include the following:

Datasets S1 to S6

www.pnas.org/cgi/doi/10.1073/pnas.1921344117

SI Materials and Methods

Bioinformatic analysis of siRNA screen data

Data analysis was automated using a custom R script which combined and analysed the CCF2-AM fluorescence (translocation ratio) and DRAQ5™ (cell viability) raw data files to generate a summarised report spreadsheet. Translocation ratio and cell viability values were normalized to the average of the siOTP-NT control readout per plate. The experimental robustness was evaluated for each screened plate using the Z' factor calculation (1), comparing the negative, positive and cell death control for both translocation ratio and cell viability. siRNA transfections that resulted in >50% average reduction in cell viability compared to siOTP-NT were scored as toxic and excluded from further analyses. Robust z-scores utilising the median and median absolute deviation (MAD) of all siOTP-NT-normalized sample values for the translocation ratio were generated across all sample wells and averaged per duplicate plate pair. Robust z-score = (sample value-sample median)/sample median absolute deviation were used as the bio-identification method (1) of which $Z \leq -2$ or $Z \geq 2$ were considered statistically significant. In the deconvolution validation screen, siRNA targets were confirmed by approximate reproduction of the translocation ratio in the primary screen and a decrease in effector translocation by 20% compared to siOTP-NT. The PANTHER Overrepresentation Test (Version 14.1; released 20190312) was used to classify the validated genes (2).

Manual siRNA transfection

HeLa cells (3920 cells/well or 19600 cells/well) were reverse transfected in 96-well and 24-well plates, respectively, with siGENOME SMARTpool siRNAs using DF1 diluted in reduced serum media for 72 h. A media change was performed 24 h post-transfection.

BlaM translocation assay

To quantify translocation of BlaM-constructs, cells were seeded into black-walled, clear bottom 96-well plates (Corning). For siRNA-treated cells, HeLa cells were seeded as described above and infected 72 h post-transfection with *C. burnetii* pBlaM-MceA or *C. burnetii* pBlaM-Cig2 at a MOI of 300. Cells were infected for 24 h, loaded with CCF2-AM using the LiveBLAzer™ FRET B/G Loading Kit (Invitrogen) and 0.1M probenecid. Translocation was measured using the CLARIOstar Microplate Reader (BMG LABTECH) and the ratio of 450 nm to 520 nm was calculated. Cells were fixed with 4% PFA for 15 min and cell viability was ascertained using DRAQ5™. Quantification of cell nuclei per well was performed from 9 fields using a 10X long WD objective on the Operetta High-Content Imaging System (Perkin Elmer) and the Find Nuclei Method B program using Harmony High Content Imaging and Analysis Software (Perkin Elmer). To induce starvation conditions, infected cells were treated 20 h post-infection with HBSS for 4 h and then subsequently loaded with the CCF2-AM fluorescent dye as described.

Real-time PCR quantification of gene silencing

Duplicate wells of siRNA treated cells seeded in 24-well plates were used to ascertain RNA silencing efficiency. At the desired time points, HeLa cells were lysed and RNA was extracted using TRIsure™ (Bioline). Quantitative Real-time PCR was performed using SsoAdvanced™ Universal SYBR® Green Supermix (Bio-Rad) from cDNA generated using the iScript™ cDNA Synthesis Kit (BioRad) following DNAse treatment (Ambion; Life Technologies). The oligonucleotide pairs used are listed in SI Appendix Table S4. Real Time PCR was performed using an Mx3005P QPCR System (Agilent Technologies) and gene expression levels were normalized to 18S rRNA expression.

Western blot analysis

Immunoblot analysis was performed as previously described (3). Membranes were blocked using 5% skim milk in Tris-buffered saline containing 0.1% Tween-20 (TBST). Primary antibodies were diluted in either 5% Bovine Serum Albumin (BSA) or skim milk in TBST and used at the following concentrations overnight at 4°C: anti-β-actin (1:5000; Sigma), anti-LRP1 (EPR3724) (1:5000; Abcam), anti-CD-M6PR (H-7) (1:100; Santa Cruz Biotechnology), anti-TPP1 (CLN2) (D-11) (1:100; Santa Cruz Biotechnology). Anti-mouse-HRP and anti-rabbit-HRP (Perkin Elmer) was used at 1:3000 and detected with Clarity™ Western ECL Blotting substrate (Bio-Rad) and the Amersham Imager 600 (GE Healthcare).

C. burnetii infections

The Quant-iT PicoGreen double stranded DNA assay kit (Thermo Fisher Scientific) was used to quantify axenically grown *C. burnetii* strains (4). Cells were infected with the appropriate MOI of *C. burnetii* and incubated for 4 h at 37°C with 5% CO_2, washed once with PBS and either fixed (bacterial entry), incubated for a further 2 h in DMEM containing 5% FCS, washed once with PBS and fixed (LAMP-1 association), or incubated in DMEM containing 5% FCS until the desired time at which point samples were either fixed for microscopy or lysed with H_2O and collected for *C. burnetii* quantification (intracellular replication). Lysed samples were pelleted and re-suspended in 100 µl of H_2O and gDNA extracted using the Quick-DNA™ Miniprep kit (Zymo Research). The number of *C. burnetii* genomes was quantified by qPCR using *ompA*-specific primers (5, 6).

Immunofluorescence and microscopy

Infected cells were fixed with 4% PFA for 15 min at appropriate time points. To discriminate between extracellular and intracellular bacteria differential staining was performed. Fixed samples were blocked in PBS containing 2% BSA (blocking buffer) prior to staining with mouse anti-*C. burnetii* (1:1000, in-house sera) followed by Alexa Fluor 488-conjugated anti-mouse antibodies (1:2000 in blocking buffer, Invitrogen). Cells were washed and fixed again before being permeabilised with PBS containing 0.1% Triton X-100 and blocked with blocking buffer. Total bacteria were stained using rabbit anti-*C. burnetii* (1:10000) followed by Alexa Fluor 568-conjugated anti-rabbit antibodies (1:2000, Invitrogen). DNA was stained with 4',6'-diamidino-2-phenylindole (DAPI)

diluted 1:10000 in PBS. Coverslips were mounted onto glass slides using ProLong Gold antifade reagent (Thermo Fisher Scientific) and quantification was performed with a Leica DMI4000b inverted microscope.

For LAMP-1 staining, fixed samples were blocked and permeabilised using blocking buffer containing 0.05% saponin. Samples were co-immunostained using mouse anti-LAMP-1 H4A3-C (1:200, DSHB) and rabbit anti-*C. burnetii* (1:10000) followed by secondary antibodies (1:2000). DNA was stained using DAPI and coverslips mounted as above. LAMP-1 association was quantified using a Leica DMI4000b inverted microscope and CCV area was determined using images acquired on a Zeiss LSM700 confocal laser scanning microscope and processed with ImageJ software.

Altered pH and media composition analysis

Stationary phase (6-7 day) cultures of luciferase-expressing *C. burnetii* were diluted to 1 × 10^7 genome equivalents (GE) in 96-well black clear-bottomed tissue culture plates (Corning) in 0.1 ml of fresh ACCM-2 medium with pH adjusted from pH 4.2 to 7.2 using HCl or NaOH. 48 h later, light production was measured by a TECAN Infinite M1000 with 500 ms integration time. For altered medium compositions, ACCM-2 was freshly prepared with components missing or additional salts and cations as indicated. 5 × 10^6 GE of stationary phase culture was diluted into 0.15 ml medium and light production was measured 48 h later.

DQ-BSA assay

HeLa cells were reverse transfected with siRNA into black-walled, clear-bottomed 96-well plates. 72 h post-transfection, media was replaced with DMEM containing 10% FCS and 10 µg/ml DQ Green BSA and incubated at 37°C in 5% CO_2 for 1 h. After incubation, wells were washed with PBS and the media replaced with 100 µl of HBSS. Lysosomal protease activity was measured using the CLARIOstar Microplate Reader at 495 nm excitation, 525 nm emission every 5 min for 2 h. The slope of the range (0-120 min) was used for analysis. Chloroquine (50µg/ml) was added 1 h prior to the addition of DQ Green BSA, when required, and remained present throughout the experiment.

RNA-seq analysis

Transcript abundances for each sample were bioinformatically quantified using kallisto (7) against a reference transcriptome (*C. burnetii* RSA 493; Accession Number AE016828.3). Differential expression analysis was performed using DESeq2 (8). After data normalisation, volcano plots (curated using Excel) were used to visualise $\log_2$(fold-change) expression data against the false discovery rate (FDR, DEseq-PADJ) and a 5% false discovery rate (FDR) cut-off was set (SI Appendix, Fig S3). Samples were omitted from further analysis if the $\log_2$(fold-change) was < 1 and > -1. The differences in gene expression profiles found in this study were compared with that of Beare *et al*. (9) using the online platform, Venny (10). Heatmaps were created using MultiexperimentViewer (MeV), version 4.8.1 (11).

Quantification and Statistical Analysis

All graphs show mean ± SEM. For comparisons between two groups an unpaired, two-tailed t-test was used. For comparisons between multiple groups either a one-way ANOVA or two-way ANOVA followed by Dunnett post-test was used as appropriate. Prism7 (GraphPad Software, Inc.) was used to perform statistical analyses, with p values less than 0.05 considered significant. Quantification of bacterial entry, LAMP-1 association and CCV area were performed blinded.

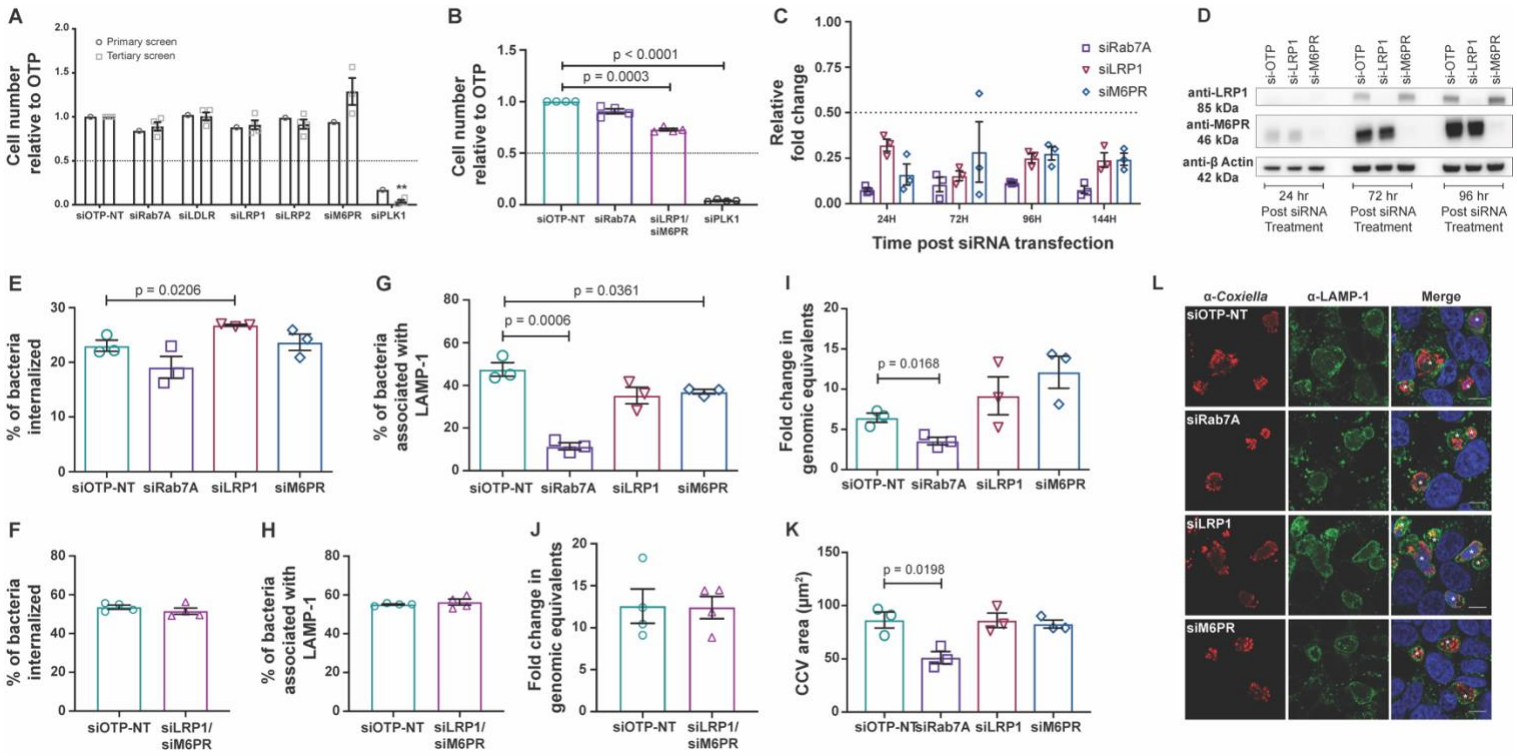
A
Cell number relative to OTP
Primary screen
Tertiary screen
siOTP-NT siRab7A siLDLR siLRP1 siLRP2 siM6PR siPLK1
B
Cell number relative to OTP
p < 0.0001
p = 0.0003
siOTP-NT siRab7A siLRP1/ siM6PR siPLK1
C
Relative fold change
siRab7A
siLRP1
siM6PR
24H 72H 96H 144H
Time post siRNA transfection
D
si-OTP si-LRP1 si-M6PR
anti-LRP1 85 kDa
anti-M6PR 46 kDa
anti-β Actin 42 kDa
24 hr Post siRNA Treatment
72 hr Post siRNA Treatment
96 hr Post siRNA Treatment
E
% of bacteria internalized
p = 0.0206
siOTP-NT siRab7A siLRP1 siM6PR
F
% of bacteria internalized
siOTP-NT siLRP1/ siM6PR
G
% of bacteria associated with LAMP-1
p = 0.0361
p = 0.0006
siOTP-NT siRab7A siLRP1 siM6PR
H
% of bacteria associated with LAMP-1
siOTP-NT siLRP1/ siM6PR
I
Fold change in genomic equivalents
p = 0.0168
siOTP-NT siRab7A siLRP1 siM6PR
J
Fold change in genomic equivalents
siOTP-NT siLRP1/ siM6PR
K
CCV area (μm²)
p = 0.0198
siOTP-NT siRab7A siLRP1 siM6PR
L
α-Coxiella
α-LAMP-1
Merge
siOTP-NT
siRab7A
siLRP1
siM6PR

Supplementary Figure 1. Using siRNA to investigate the role of specific lysosomal receptors during *C. burnetii* infection. (A and B) HeLa cells used in the translocation assay (Figure 2A and 2B) were subsequently fixed and stained with DRAQ5™ to determine cell viability. Results are expressed relative to non-targeting control (siOTP-NT) with error bars indicating SEM from at least three independent experiments. Statistical difference between tested siRNA and siOTP-NT was determined using one-way ANOVA, followed by Dunnett's multiple comparison post-test on raw data. ** $p < 0.01$. The dotted line indicates a cell viability of 0.5 relative to siOTP-NT. The outcome from the primary screen (circles) are also shown for comparison in part A. (C) qRT-PCR measuring mRNA levels of Rab7A, LRP1 and M6PR in HeLa cells at the indicated times post siRNA transfection. Results are normalized to 18S rRNA and displayed as fold change relative to siOTP-NT-treated cells. A four-fold reduction in *LRP1* and *M6PR* mRNA compared to siOTP-NT treated HeLa cells over the total duration of experiments was observed. (D) The absence of protein expression was confirmed by immunoblot analysis of cell lysates from HeLa cells treated with siRNA SMARTpools collected at 24, 72 and 96 h post siRNA treatment using anti-LRP1 (top panel) and anti-M6PR (middle panel) antibodies. Anti-β Actin was used as a loading control (bottom panel). (E-L) The impact of silencing *LRP1* or *M6PR* on *C. burnetii* infection was established either individually (E, G, I, K and L) or in combination (F, H and J) with *RAB7A* siRNA treatment used as a control. (E and F) Bacterial entry was ascertained in HeLa cells treated with siRNA SMARTpools for 72 h and infected with *C. burnetii* at a MOI of 100 for 4 h. Differential intracellular/extracellular staining was performed and at least 200 cell-associated bacteria were quantified per experiment.

Results are expressed as the mean percentage of internalized bacteria with no decrease in bacterial ingress observed compared to siOTP-NT treated cells. (G and H) Bacterial association with the lysosomal marker LAMP-1 was determined in HeLa cells treated with siRNA SMARTpools and infected with *C. burnetii* at a MOI of 100 for 6 h. Cells were fixed and stained with anti-LAMP-1 and anti-*Coxiella* antibodies. The localisation of LAMP-1 around at least 150 internalized bacteria was evaluated per experiment and results are expressed as the mean percentage of bacteria positively associated with LAMP-1. The slight reduction in *LRP1* (35%) and *M6PR* (37%) depleted cells was not as severe as observed in siRab7A treated cells in which progression to the lysosome is halted and only 11% of bacteria associated with LAMP-1. (I and J) Intracellular replication of *C. burnetii* in HeLa cells treated with siRNA SMARTpools and infected with *C.burnetii* at a MOI of 50 for 72 h. Results are presented as the fold-increase in genome equivalents three days post-infection relative to the inoculum as determined by *ompA*-specific qPCR. (K) The area of *C. burnetii* CCVs was determined in HeLa cells treated with siRNA SMARTpools and subsequently infected with *C. burnetii* at a MOI of 50 for 3 days. At least 50 CCV were measured per experiment and results are expressed as the average CCV area (μm^2) from at least three experiments. Error bars represent SEM and statistical difference between siOTP-NT and tested siRNA was determined using an un-paired, two-tailed t-test on raw data. As expected, the decrease in LAMP-1 association correlated with a reduction in bacterial replication and vacuole size in *RAB7A* depleted HeLa cells infected with *C. burnetii* for 3 days with no reduction observed in other siRNA treatments. (L) Representative confocal micrograph images of siRNA treated HeLa cells infected for 3 days with *C. burnetii* used to quantify CCV area in part K. Cells

were stained with anti-*Coxiella* antibody (red), anti-LAMP-1 antibody (green) and DAPI (blue). Scale bars represent 10 µm. Asterisk indicates CCV.

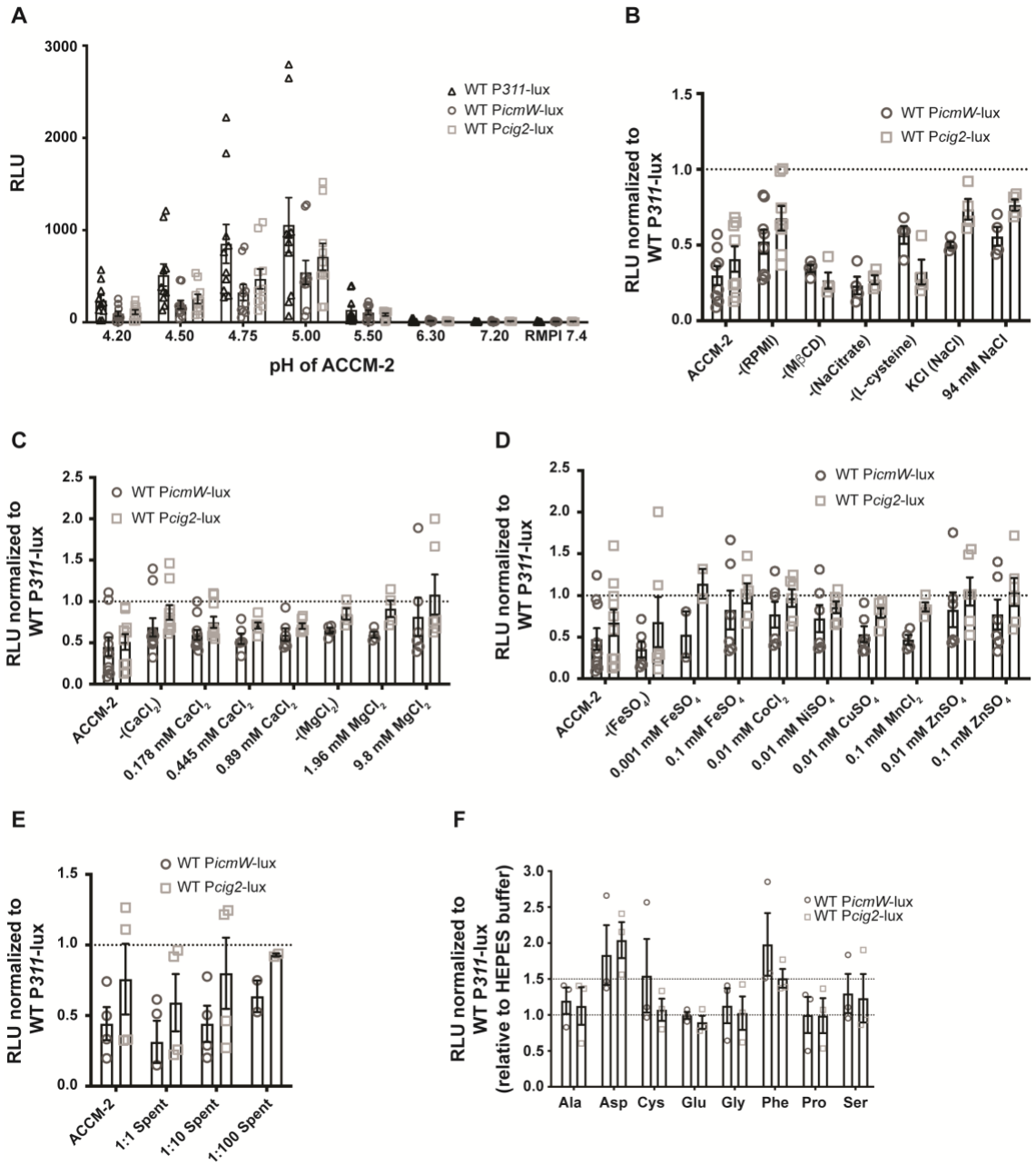

Supplementary Figure 2. Altered pH and media composition does not specifically alter PmrA regulated gene transcription. (A) Light production by $1 \times 10_7$ GE of *C. burnetii* strains expressing bacterial luciferase activated by control (P*311*) or

PmrA-dependent (P*icmW* or P*cig2*) promoters 48 h after inoculation into ACCM-2 or RPMI with pH adjusted as indicated. Data is presented as RLU (relative light units) with error bars representing SEM from five independent experiments. (B-E) Light production by PmrA-regulated *icmW* and *cig2* promoters 48 h after inoculation of 5×10^7 GE into ACCM-2 with noted dropouts or substitutions (B, in parentheses) and modifications of Ca^{2+}/Mg^{2+} concentration (C), divalent cations (D) and spent media addition (E). Data is presented as RLU relative to the control (P*311*-lux) with error bars representing SEM from at least two independent experiments. Statistical difference between alterations and ACCM-2 for either P*icmW*-lux (circle) or P*cig2*-lux (square) was determined using two-way ANOVA, followed by Dunnett's multiple comparison post-test on raw data following normalisation to P*311*-lux. (F) Axenic *C. burnetii* strains expressing bacterial luciferase reporters were grown for 72 h prior to the addition of 10 mM of different amino acids for 20 min. Data is presented as RLU relative to addition of HEPES buffer alone and normalized to P*311*-lux with error bars representing SEM from three independent experiments. Statistical difference between P*311*-lux and P*icmW*-lux (circle) or P*cig2*-lux (square) was determined using two-way ANOVA, followed by Dunnett's multiple comparison post-test.

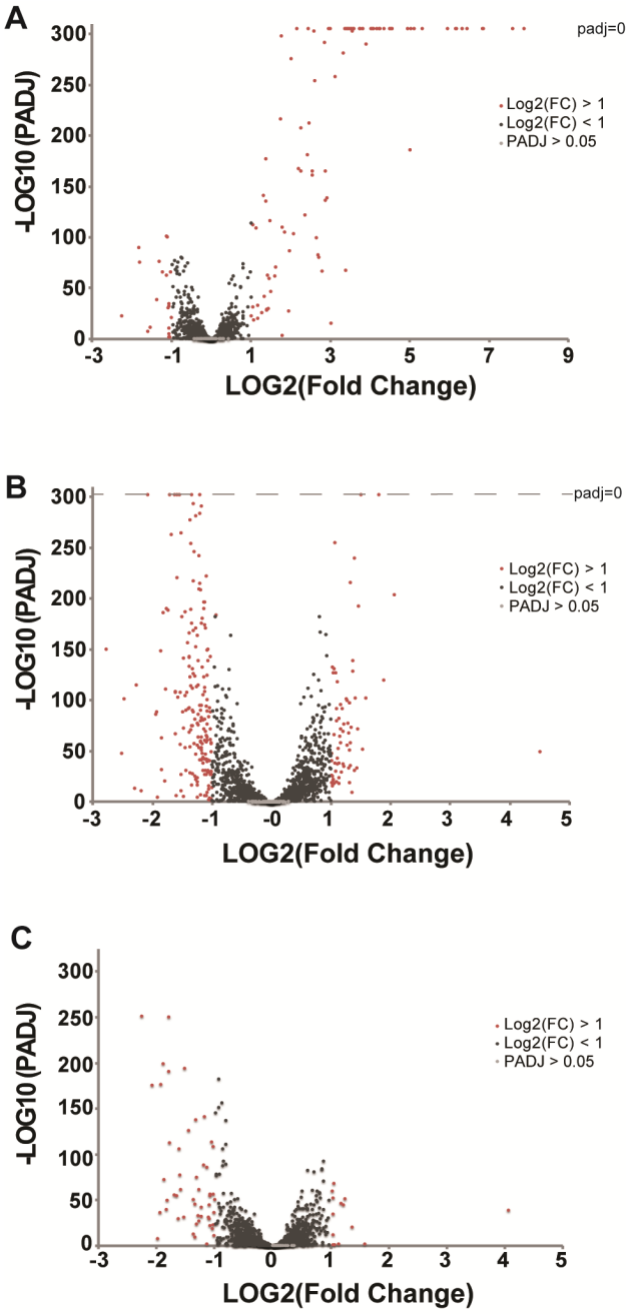

Supplementary Figure 3. Global changes in *C. burnetii* gene expression, comparing WT and *pmrA*::Tn in the presence of water (H_2O) or amino acids (AA). Volcano plots illustrate the distribution of change (log2(fold change (FC))) detected against

significance, *p*-value adjusted for multiple testing using Benjamini-Hochberg to estimate the false discovery rate (PADJ). (A) WT H_2O versus *pmrA*::Tn H_2O, (B) WT AA versus WT H_2O, (C) *pmrA*::Tn AA versus *pmrA*::Tn H_2O. Log2(FC) > 1 are shown in red, log2(FC) < 1 are black and comparisons with insignificant PADJ value (> 0.05) are shown in grey. Changes in expression that have PADJ values of zero are indicated by a dashed line.

Table S1: Summary of statistically significant biological processes that were overrepresented in the 251 validated targets. Includes both child and parent PANTHER GO-Slim Biological Process categories alongside p-values calculated using Fisher's exact test and the False Discovery Rate (FDR) calculated using the Benjamini-Hochberg procedure.

PANTHER GO-SLIM Biological Process (parent categories)	**Homo sapiens (REF) #**	**Validated targets #**	**Expected**	**Fold Enrichment**	**+/-**	**raw P value**	**FDR**
C-terminal protein amino acid modification	3	2	0.03	67.95	+	9.22E-04	2.81E-02
↳cellular process	6070	83	59.56	1.39	+	4.96E-04	1.62E-02
intra-Golgi vesicle-mediated transport	28	9	0.27	32.76	+	6.37E-11	9.53E-09
↳Golgi vesicle transport	124	19	1.22	15.62	+	1.83E-16	5.48E-14
↳vesicle-mediated transport	643	38	6.31	6.02	+	1.76E-18	7.90E-16
↳transport	1255	56	12.31	4.55	+	1.10E-21	6.58E-19
↳establishment of localization	1255	56	12.31	4.55	+	1.10E-21	9.87E-19
↳localization	2059	76	20.2	3.76	+	4.39E-25	7.89E-22
activation of JUN kinase activity	10	3	0.1	30.58	+	2.41E-04	8.82E-03
↳regulation of macromolecule metabolic process	112	6	1.1	5.46	+	1.05E-03	3.08E-02
↳positive regulation of protein kinase activity	60	6	0.59	10.19	+	4.37E-05	2.31E-03
↳activation of protein kinase activity	57	6	0.56	10.73	+	3.35E-05	1.82E-03
↳JNK cascade	44	4	0.43	9.27	+	1.21E-03	3.44E-02
↳stress-activated MAPK cascade	45	4	0.44	9.06	+	1.30E-03	3.60E-02
↳intracellular signal transduction	777	20	7.62	2.62	+	1.05E-04	4.49E-03
↳stress-activated protein kinase signaling cascade	43	4	0.42	9.48	+	1.11E-03	3.23E-02
activation of MAPKK activity	20	5	0.2	25.48	+	3.74E-06	2.92E-04
divalent metal ion transport	37	7	0.36	19.28	+	2.09E-07	2.50E-05
↳metal ion transport	49	7	0.48	14.56	+	1.14E-06	1.03E-04
↳cation transport	105	8	1.03	7.77	+	1.48E-05	9.86E-04
↳ion transport	186	8	1.82	4.38	+	6.38E-04	2.05E-02
↳divalent inorganic cation transport	37	7	0.36	19.28	+	2.09E-07	2.34E-05
cellular divalent inorganic cation homeostasis	27	5	0.26	18.87	+	1.34E-05	9.27E-04
↳regulation of biological quality	643	17	6.31	2.69	+	2.60E-04	9.33E-03
transition metal ion transport	41	7	0.4	17.4	+	3.88E-07	4.10E-05
retrograde transport, endosome to Golgi	33	5	0.32	15.44	+	3.19E-05	1.91E-03
↳intracellular transport	133	7	1.3	5.36	+	4.46E-04	1.54E-02
↳cellular localization	934	44	9.16	4.8	+	8.54E-18	3.07E-15
↳cytosolic transport	36	5	0.35	14.16	+	4.65E-05	2.39E-03
transition metal ion homeostasis	49	7	0.48	14.56	+	1.14E-06	1.08E-04
↳metal ion homeostasis	69	8	0.68	11.82	+	8.21E-07	8.19E-05
ER to Golgi vesicle-mediated transport	84	12	0.82	14.56	+	1.57E-10	2.17E-08
synaptic vesicle exocytosis	36	5	0.35	14.16	+	4.65E-05	2.32E-03
↳synaptic signaling	331	12	3.25	3.7	+	1.42E-04	5.41E-03
↳synaptic vesicle cycle	26	5	0.26	19.6	+	1.14E-05	8.20E-04
↳neurotransmitter secretion	66	5	0.65	7.72	+	6.38E-04	2.01E-02
↳chemical synaptic transmission	330	12	3.24	3.71	+	1.38E-04	5.62E-03
↳anterograde trans-synaptic signaling	330	12	3.24	3.71	+	1.38E-04	5.50E-03

↳trans-synaptic signaling	331	12	3.25	3.7	+	1.42E-04	5.53E-03
↳organelle localization	77	8	0.76	10.59	+	1.76E-06	1.50E-04
organelle localization by membrane tethering	39	5	0.38	13.07	+	6.58E-05	3.11E-03
cellular metal ion homeostasis	43	5	0.42	11.85	+	1.01E-04	4.41E-03
Ras protein signal transduction	139	16	1.36	11.73	+	2.55E-12	4.17E-10
↳small GTPase mediated signal transduction	147	17	1.44	11.79	+	4.82E-13	8.66E-11
regulation of exocytosis	50	5	0.49	10.19	+	1.93E-04	7.24E-03
↳regulation of vesicle-mediated transport	62	5	0.61	8.22	+	4.89E-04	1.63E-02
lipid transport	83	8	0.81	9.82	+	2.95E-06	2.41E-04
↳lipid localization	92	8	0.9	8.86	+	6.00E-06	4.49E-04
↳macromolecule localization	172	9	1.69	5.33	+	7.21E-05	3.32E-03
synaptic transmission, glutamatergic	44	4	0.43	9.27	+	1.21E-03	3.38E-02
response to metal ion	47	4	0.46	8.67	+	1.51E-03	4.12E-02
inorganic cation transmembrane transport	84	7	0.82	8.49	+	3.00E-05	1.86E-03
↳ion transmembrane transport	85	7	0.83	8.39	+	3.22E-05	1.86E-03
↳inorganic ion transmembrane transport	85	7	0.83	8.39	+	3.22E-05	1.81E-03
regulation of gene expresssion	72	5	0.71	7.08	+	9.24E-04	2.77E-02
vesicle fusion to plasma membrane	116	8	1.14	7.03	+	2.91E-05	1.87E-03
↳vesicle fusion	22	4	0.22	18.53	+	1.09E-04	4.57E-03
↳membrane fusion	138	8	1.35	5.91	+	9.29E-05	4.17E-03
↳membrane organization	378	12	3.71	3.24	+	4.56E-04	1.54E-02
↳plasma membrane fusion	125	8	1.23	6.52	+	4.81E-05	2.33E-03
protein targeting	84	5	0.82	6.07	+	1.77E-03	4.74E-02
↳intracellular protein transport	714	37	7.01	5.28	+	2.94E-16	7.55E-14
↳cellular protein localization	853	40	8.37	4.78	+	3.94E-16	8.84E-14
↳cellular macromolecule localization	857	40	8.41	4.76	+	4.58E-16	9.14E-14
receptor-mediated endocytosis	103	6	1.01	5.94	+	6.90E-04	2.14E-02
↳endocytosis	314	11	3.08	3.57	+	3.55E-04	1.25E-02
Unclassified	10588	64	103.88	0.62	-	3.26E-08	4.18E-06

Table S2: Targets that have been experimentally verified as either exclusive or partial lysosomal localisation (12). Targets are ranked according to the translocation ratio outcome from the primary screen. Targets selected for the validation screen are noted alongside the outcome from the validation screen. **Green fill indicates normalised ratio ≤ 0.8.**

Entrez gene name	Description	Genbank Accession number	Average cell count normalised to OTP	Average ratio normalised to OTP	Validation screen	Level of confidence
ATP6V0C	ATPase, H+ transporting, lysosomal 16kDa, V0 subunit c	NM_001694	0.85	**0.26**	Yes	Moderate-confidence (2/4)
ATP6V1E1	ATPase, H+ transporting, lysosomal 31kDa, V1 subunit E1	NM_001039367	0.99	**0.3**	Yes	High-confidence (4/4)
FLJ10815	solute carrier family 38, member 7	NM_018231	0.78	**0.36**	Yes	Did not validate
KIAA1001	arylsulfatase G	NM_014960	1.01	**0.44**		
CLN2	tripeptidyl peptidase I	NM_000391	1.03	**0.46**		
PTTG1IP	pituitary tumor-transforming 1 interacting protein	NM_004339	1.01	**0.48**		
SPPL2A	signal peptide peptidase-like 2A	NM_032802	1.09	**0.48**		
ATP6V0A1	ATPase, H+ transporting, lysosomal V0 subunit a1	NM_005177	1.05	**0.49**		
ATP6A	ATPase, H+	NM_0011	0.9	**0.5**		

P1	transporting, lysosomal accessory protein 1	83				
HEXA	hexosaminidase A (alpha polypeptide)	NM_000520	0.97	**0.5**		
FLJ20014	chromosome 17 open reading frame 59	NM_017622	0.65	**0.52**		
PPGB	cathepsin A	NM_000308	1.12	**0.52**	Yes	Did not validate
ATP6V1A	ATPase, H+ transporting, lysosomal 70kDa, V1 subunit A	NM_001690	0.93	**0.53**		
ATP6V1C1	ATPase, H+ transporting, lysosomal 42kDa, V1 subunit C1	NM_001695	0.98	**0.53**		
HPSE	heparanase	NM_001098540	0.99	**0.53**		
PSAP	prosaposin	NM_002778	0.98	**0.53**		
CD63	CD63 molecule	NM_001040034	1	**0.54**		
CTSF	cathepsin F	NM_003793	0.96	**0.54**	Yes	Did not validate
FLJ20507	transmembrane protein 127	NM_017849	0.94	**0.54**	Yes	Moderate-confidence (2/4)
GNS	glucosamine (N-acetyl)-6-sulfatase	NM_002076	1.08	**0.55**		
GALNS	galactosamine (N-acetyl)-6-sulfate sulfatase	NM_000512	0.93	**0.56**		
RRAG	Ras-related	NM_0065	1.12	**0.57**	Yes	Did not

A	GTP binding A	70				validate
TPCN2	two pore segment channel 2	NM_139075	0.84	**0.57**		
CTSO	cathepsin O	NM_001334	1.04	**0.58**	Yes	Did not validate
MANBA	mannosidase, beta A, lysosomal	NM_005908	1	**0.58**	Yes	High-confidence (4/4)
FLJ30668	transmembrane protein 74	NM_153015	0.9	**0.58**	Yes	Moderate-confidence (2/4)
CTSC	cathepsin C	NM_001814	1.14	**0.59**	Yes	High-confidence (3/4)
ARL10B	ADP-ribosylation factor-like 8A	NM_138795	0.92	**0.6**		
LAPTM4B	lysosomal protein transmembrane 4 beta	NM_018407	0.92	**0.6**	Yes	Did not validate
LAPTM5	lysosomal protein transmembrane 5	NM_006762	0.88	**0.61**	Yes	Did not validate
ATP6V0E	ATPase, H+ transporting, lysosomal 9kDa, V0 subunit e1	NM_003945	0.87	**0.62**		
ATP6V1H	ATPase, H+ transporting, lysosomal 50/57kDa, V1 subunit H	NM_213620	0.5	**0.62**		
SCARB2	scavenger receptor class B, member 2	NM_005506	0.96	**0.62**		
SIDT2	SID1 transmembrane family,	NM_001040455	0.99	**0.62**		

	member 2					
NEU1	sialidase 1 (lysosomal sialidase)	NM_000434	0.93	**0.63**	Yes	Moderate-confidence (2/4)
FUCA1	fucosidase, alpha-L- 1, tissue	NM_000147	0.94	**0.64**		
CLCN7	chloride channel 7	NM_001287	0.92	**0.65**		
ARL10C	ADP-ribosylation factor-like 8B	NM_018184	1.12	**0.66**		
CTSS	cathepsin S	NM_004079	1.02	**0.66**	Yes	Did not validate
NPC2	Niemann-Pick disease, type C2	NM_006432	1.19	**0.66**	Yes	High-confidence (3/4)
HYAL2	hyaluronoglucosaminidase 2	NM_003773	0.84	**0.67**		
C20ORF103	chromosome 20 open reading frame 103	NM_012261	1.23	**0.68**		
LIPA	lipase A, lysosomal acid, cholesterol esterase	NM_000235	1.1	**0.68**	Yes	Did not validate
ASAHL	N-acylethanolamine acid amidase	NM_001042402	1.07	**0.68**		
MGC33302	major facilitator superfamily domain containing 8	NM_152778	0.97	**0.69**		
NEU4	sialidase 4	NM_080741	0.97	**0.69**		
CTSB	cathepsin B	NM_001908	1.14	**0.7**	Yes	Moderate-confidence (2/4)

DEPDC6	DEP domain containing MTOR-interacting protein	NM_022783	0.9	**0.7**		
C7ORF28A	CCZ1 vacuolar protein trafficking and biogenesis associated homolog (S. cerevisiae)	NM_015622	1.01	**0.71**		
CTNS	cystinosin, lysosomal cystine transporter	NM_001031681	0.9	**0.71**	Yes	Moderate-confidence (2/4)
EPDR1	ependymin related protein 1 (zebrafish)	NM_017549	0.9	**0.71**		
LGMN	legumain	NM_005606	1.13	**0.72**	Yes	Did not validate
AGA	aspartylglucosaminidase	NM_000027	0.87	**0.73**		
C2ORF28	chromosome 2 open reading frame 28	NM_016085	1.12	**0.73**		
NAGLU	N-acetylglucosaminidase, alpha	NM_000263	0.93	**0.73**		
MPO	myeloperoxidase	NM_000250	0.98	**0.74**		
NPC1	Niemann-Pick disease, type C1	NM_000271	0.92	**0.74**	Yes	High-confidence (4/4)
SLC26A11	solute carrier family 26, member 11	NM_173626	0.96	**0.74**	Yes	Moderate-confidence (2/4)
SLC37A3	solute carrier family 37 (glycerol-3-phosphate	NM_032295	1	**0.74**		

	transporter), member 3					
MGC4618	transmembrane protein 175	NM_032326	1.09	**0.74**	Yes	Moderate-confidence (2/4)
ATP6V1F	ATPase, H+ transporting, lysosomal 14kDa, V1 subunit F	NM_004231	0.96	**0.76**		
PRCP	prolylcarboxypeptidase (angiotensinase C)	NM_005040	1.05	**0.76**		
FLJ90709	solute carrier family 38, member 9	NM_173514	1.06	**0.76**		
CTBS	chitobiase, di-N-acetyl-	NM_004388	1.01	**0.77**		
PQLC2	PQ loop repeat containing 2	NM_001040126	1.09	**0.77**		
TDE2L	serine incorporator 2	NM_178865	1.02	**0.77**		
HEXB	hexosaminidase B (beta polypeptide)	NM_000521	0.96	**0.78**		
GM2A	GM2 ganglioside activator	NM_000405	1.08	**0.8**		
RHEB	Ras homolog enriched in brain	NM_005614	1	**0.8**		
C2ORF18	chromosome 2 open reading frame 18	NM_017877	1.06	**0.8**		
LOC283537	solute carrier family 46, member 3	NM_181785	0.92	**0.8**		
TSC2	tuberous sclerosis 2	NM_001077183	1.21	**0.8**		
FRAP1	mechanistic target of	NM_004958	0.94	**0.81**		

	rapamycin (serine/threonine kinase)					
ABCD4	ATP-binding cassette, sub-family D (ALD), member 4	NM_005050	0.97	**0.82**		
ATP6V0D1	ATPase, H+ transporting, lysosomal 38kDa, V0 subunit d1	NM_004691	0.94	**0.82**		
CTSD	cathepsin D	NM_001909	1.1	**0.82**	Yes	Did not validate
GBA	glucosidase, beta, acid	NM_000157	0.94	**0.82**		
IFI30	interferon, gamma-inducible protein 30	NM_006332	0.88	**0.82**		
FLJ38482	transmembrane protein 192	NM_001100389	1.13	**0.82**		
ATP6V1G1	ATPase, H+ transporting, lysosomal 13kDa, V1 subunit G1	NM_004888	1.1	**0.83**		
ARSA	arylsulfatase A	NM_001085428	0.96	**0.84**		
MGC31963	chromosome 1 open reading frame 85	NM_144580	0.88	**0.84**		
PGCP	plasma glutamate carboxypeptidase	NM_016134	1.18	**0.84**		
LOH12CR1	loss of heterozygosity, 12, chromosomal region 1	NM_058169	1.01	**0.86**		
NCSTN	nicastrin	NM_015331	0.98	**0.86**		

MGC3265	prenylcysteine oxidase 1 like	NM_024028	0.9	**0.86**		
ACP2	acid phosphatase 2, lysosomal	NM_001610	0.98	**0.87**		
BCL2L11	BCL2-like 11 (apoptosis facilitator)	NM_207002	1.04	**0.87**		
PPT2	palmitoyl-protein thioesterase 2	NM_005155	0.9	**0.87**		
MAPBPIP	late endosomal/lysosomal adaptor, MAPK and MTOR activator 2	NM_014017	0.26	**0.88**		
MCRS1	microspherule protein 1	NM_006337	0.9	**0.88**		
KIAA0602	phosphofurin acidic cluster sorting protein 2	NM_015197	1.05	**0.88**		
TPCN1	two pore segment channel 1	NM_017901	0.98	**0.88**		
ATP6V1D	ATPase, H+ transporting, lysosomal 34kDa, V1 subunit D	NM_015994	1.04	**0.89**		
C10ORF32	chromosome 10 open reading frame 32	NM_144591	0.84	**0.89**		
FYCO1	FYVE and coiled-coil domain containing 1	NM_024513	1.14	**0.89**		
GUSB	glucuronidase, beta	NM_000181	1.04	**0.89**		
MCOLN1	mucolipin 1	NM_020533	0.98	**0.89**	Yes	Did not validate

SLC17A5	solute carrier family 17 (anion/sugar transporter), member 5	NM_012434	0.99	**0.89**		
CD68	CD68 molecule	NM_001040059	1.04	**0.9**		
GAA	glucosidase, alpha; acid	NM_001079804	0.92	**0.9**		
GZMA	granzyme A (granzyme 1, cytotoxic T-lymphocyte-associated serine esterase 3)	NM_006144	0.48	**0.9**		
PPT1	palmitoyl-protein thioesterase 1	NM_000310	1.09	**0.9**		
SMPD1	sphingomyelin phosphodiesterase 1, acid lysosomal	NM_001007593	0.98	**0.9**		
TTYH3	tweety homolog 3 (Drosophila)	NM_025250	0.93	**0.9**		
ABCA2	ATP-binding cassette, sub-family A (ABC1), member 2	NM_001606	1.04	**0.91**		
CPVL	carboxypeptidase, vitellogenic-like	NM_031311	1.04	**0.91**		
C6ORF209	LMBR1 domain containing 1	NM_018368	0.98	**0.91**		
DKFZP313G1735	arylsulfatase family, member K	NM_198150	1.01	**0.92**		
CTSL	cathepsin L1	NM_145918	1.09	**0.92**		
GGH	gamma-	NM_0038	1.06	**0.92**		

	glutamyl hydrolase (conjugase, folylpolygammaglutamyl hydrolase)	78				
LAMP3	lysosomal-associated membrane protein 3	NM_014398	1.14	**0.92**		
LYPLA3	phospholipase A2, group XV	NM_012320	0.99	**0.92**		
REN	renin	NM_000537	0.8	**0.92**		
TSPAN-1	tetraspanin 1	NM_005727	0.96	**0.92**		
BAX	BCL2-associated X protein	NM_138763	0.91	**0.93**		
GZMB	granzyme B (granzyme 2, cytotoxic T-lymphocyte-associated serine esterase 1)	NM_004131	0.98	**0.93**		
CTSZ	cathepsin Z	NM_001336	0.9	**0.94**		
CSE-C	sialic acid acetylesterase	NM_170601	1	**0.94**		
LOC389541	chromosome 7 open reading frame 59	NM_001008395	0.87	**0.96**		
OSTM1	osteopetrosis associated transmembrane protein 1	NM_014028	1.08	**0.96**		
RRAGB	Ras-related GTP binding B	NM_006064	0.97	**0.96**		
TMEM8	transmembrane protein 8A	NM_021259	1.02	**0.96**		
ATP6V1B2	ATPase, H+ transporting,	NM_001693	0.92	**0.98**		

	lysosomal 56/58kDa, V1 subunit B2					
MFSD1	major facilitator superfamily domain containing 1	NM_022736	1.05	**0.98**		
SNAPAP	SNAP-associated protein	NM_012437	1.17	**0.98**		
TM6SF1	transmembrane 6 superfamily member 1	NM_023003	1.06	**0.98**		
ABCB6	ATP-binding cassette, sub-family B (MDR/TAP), member 6	NM_005689	0.96	**0.99**		
LGALS3	lectin, galactoside-binding, soluble, 3	NM_002306	0.7	**0.99**		
LAMP2	lysosomal-associated membrane protein 2	NM_002294	1.13	**1**		
ABCB9	ATP-binding cassette, sub-family B (MDR/TAP), member 9	NM_019624	0.61	**1.01**		
CTSH	cathepsin H	NM_148979	0.98	**1.02**		
HYAL1	hyaluronoglucosaminidase 1	NM_007312	1.12	**1.02**		
MARCH8	membrane-associated ring finger (C3HC4) 8	NM_001002266	1.02	**1.02**		
GBL	MTOR associated	NM_022372	0.97	**1.02**		

	protein, LST8 homolog (S. cerevisiae)					
RRAGD	Ras-related GTP binding D	NM_021244	0.62	**1.02**		
SGSH	N-sulfoglucosamine sulfohydrolase	NM_000199	1.1	**1.02**		
MAP2K1IP1	late endosomal/lysosomal adaptor, MAPK and MTOR activator 3	NM_021970	1.09	**1.03**		
SLC36A1	solute carrier family 36 (proton/amino acid symporter), member 1	NM_078483	1.1	**1.04**		
MEF2B	MEF2BNB-MEF2B readthrough	NM_005919	0.93	**1.05**		
APCS	amyloid P component, serum	NM_001639	1.01	**1.06**		
NAGA	N-acetylgalactosaminidase, alpha-	NM_000262	1	**1.06**		
CREG	cellular repressor of E1A-stimulated genes 1	NM_003851	1.06	**1.07**		
DNASE2	deoxyribonuclease II, lysosomal	NM_001375	1.05	**1.07**		
MAN2B2	mannosidase, alpha, class 2B, member 2	NM_015274	0.98	**1.07**		
AKT1S	AKT1 substrate	NM_0010	1.04	**1.08**		

1	1 (proline-rich)	98633				
IDUA	iduronidase, alpha-L-	NM_000203	0.98	**1.08**		
GLB1	galactosidase, beta 1	NM_001079811	0.96	**1.1**		
MAN2B1	mannosidase, alpha, class 2B, member 1	NM_000528	1.12	**1.1**		
SLC37A2	solute carrier family 37 (glycerol-3-phosphate transporter), member 2	NM_198277	1.12	**1.1**		
SCPEP1	serine carboxypeptidase 1	NM_021626	1	**1.11**		
ACP5	acid phosphatase 5, tartrate resistant	NM_001611	0.98	**1.12**		
RNASET2	ribonuclease T2	NM_003730	1.02	**1.12**		
TTYH2	tweety homolog 2 (Drosophila)	NM_052869	1.1	**1.12**		
DIRC2	disrupted in renal carcinoma 2	NM_032839	0.96	**1.14**		
PLD3	phospholipase D family, member 3	NM_012268	1.07	**1.14**		
DPP7	dipeptidyl-peptidase 7	NM_013379	1.02	**1.15**		
CTSK	cathepsin K	NM_000396	1.07	**1.16**		
C14ORF9	transmembrane protein 55B	NM_144568	1.02	**1.16**		
TM7SF1	G protein-coupled receptor 137B	NM_003272	1.04	**1.19**		
BLOC1S1	biogenesis of lysosomal	NM_001487	0.98	**1.2**		

	organelles complex-1, subunit 1					
ASAH1	N-acylsphingosine amidohydrolase (acid ceramidase) 1	NM_004315	0.86	**1.21**		
BLOC1S2	biogenesis of lysosomal organelles complex-1, subunit 2	NM_001001342	1.06	**1.21**		
GALC	galactosylceramidase	NM_001037525	1.06	**1.21**		
IDS	iduronate 2-sulfatase	NM_006123	1	**1.21**		
ARSB	arylsulfatase B	NM_198709	1.06	**1.23**		
LYSAL1	ectonucleoside triphosphate diphosphohydrolase 4	NM_004901	1.03	**1.23**		
GLA	galactosidase, alpha	NM_000169	0.84	**1.23**		
IL4I1	interleukin 4 induced 1	NM_152899	1.06	**1.23**		
LITAF	lipopolysaccharide-induced TNF factor	NM_004862	0.83	**1.27**		
HBXIP	hepatitis B virus x interacting protein	NM_006402	1.1	**1.31**		
MGC2749	chromosome 19 open reading frame 50	NM_024069	1.19	**1.36**		
RRAGC	Ras-related GTP binding C	NM_022157	1.03	**1.37**		
TMEM9	transmembrane protein 9	NM_016456	0.97	**1.37**		

LGALS8	lectin, galactoside-binding, soluble, 8	NM_201545	1.06	**1.38**		
FLJ20255	transmembrane protein 104	NM_017728	0.9	**1.4**		
CLN3	ceroid-lipofuscinosis, neuronal 3	NM_000086	0.87	**1.42**		
LOC196463	phospholipase B domain containing 2	NM_173542	0.92	**1.47**		
LAMP1	lysosomal-associated membrane protein 1	NM_005561	1.19	**1.48**		
LAPTM4A	lysosomal protein transmembrane 4 alpha	NM_014713	0.42	**1.58**		
CLN5	ceroid-lipofuscinosis, neuronal 5	NM_006493	0.73	**1.62**		
Raptor	regulatory associated protein of MTOR, complex 1	NM_020761	0.87	**1.62**		
AOAH	acyloxyacyl hydrolase (neutrophil)	NM_001637	0.23	**1.71**		
FLJ20625	late endosomal/lysosomal adaptor, MAPK and MTOR activator 1	NM_017907	0.98	**1.97**		

Table S3: List of genes significantly upregulated in *C. burnetii* WT compared to *C. burnetii pmrA*::Tn in both Beare *et al* (9) and this study. Experimentally verified effectors are indicated. From the unique cohort of genes in this study, those that have been previously identified as effectors are highlighted in bold.

Genes specific to Beare *et al*.			**Genes common in both studies**			**Genes specific to this study**	
CBU0062	Known effector(13)		CBU0021	Known effector(14-16)		CBU0222	
CBU0077	Known effector(17, 18)		CBU0041	Known effector(19, 20)		CBU0027	
CBU0113	Known effector(13, 20)		CBU0049			CBU0086	
CBU0122	Known effector(9)		CBU0084			CBU0119	
CBU0210			CBU0273			CBU0339	
CBU0215			CBU0343			CBU0617	
CBU0306			CBU0388	Known effector(15, 20)		CBU0618	
CBU0372	Known effector(20)		CBU0409			CBU0619	
CBU0439			CBU0410	Known effector(19, 20)		CBU0731	
CBU0440			CBU0436			CBU0789	
CBU0624			CBU0505			CBU0793	
CBU0634			CBU0508			**CBU0794**	Known effector(19, 20)
CBU0635	Known effector(17)		CBU0560			**CBU0881**	Known effector(19, 20)
CBU0658			CBU0665	Known effector(20, 21)		**CBU1198**	Known effector(20)

CBU0705			CBU0786			CBU1199	
CBU0706			CBU0802			**CBU1213**	Known effector(22)
CBU0707			CBU0860			CBU1214	
CBU0742			CBU1063	Known effector(13)		CBU1291	
CBU0787			CBU1098			CBU1292	
CBU0967			CBU1103			**CBU1409**	Known effector(13)
CBU0970			CBU1228			CBU1477	
CBU1041			CBU1314	Known effector(19, 20)		CBU1478	
CBU1152			CBU1366			CBU1493	
CBU1209	Predicted effector(13)		CBU1369			CBU1612	
CBU1227			CBU1370	Known effector(13)		CBU1613	
CBU1230			CBU1387	Known effector(13)		CBU1618	
CBU1231			CBU1457	Known effector(19, 20)		CBU1647	
CBU1279a			CBU1530	Known effector(9)		CBU1701	Predicted effector(13)
CBU1529			CBU1543	Known effector(19, 20)		CBU1753	
CBU1540			CBU1556	Known effector(14, 19, 20)		**CBU1780**	Known effector(16)
CBU1621			CBU1614	Known effector(9)		**CBU1823**	Known effector(17, 19, 20)
CBU1686	Known effector(9, 15)		CBU1622			**CBU1825**	Known effector(17, 19, 20)
CBU1733			CBU1623			CBU1936	
CBU1758b			CBU1624			CBU2015a	
CBU1824			CBU1625			**CBUA0014**	Known effector(23)
CBU1948			CBU1626			**CBUA0016**	Known effector(23)

CBU2056	Known effector(17)		CBU1627				
			CBU1628				
			CBU1629				
			CBU1630				
			CBU1631				
			CBU1632				
			CBU1633				
			CBU1634				
			CBU1634a	Known effector(13)			
			CBU1636	Known effector(19, 20)			
			CBU1643				
			CBU1644				
			CBU1645				
			CBU1646				
			CBU1648				
			CBU1649				
			CBU1650				
			CBU1651				
			CBU1652				
			CBU1685	Known effector(9, 20)			
			CBU1751	Known effector(19, 20)			
			CBU1752	Known effector(9)			
			CBU1794	Known effector(13)			
			CBU1863	Known effector(14)			
			CBU2052	Known effector(17, 19, 20)			
			CBUA0015	Known effector(23)			

Table S4: List of strains, plasmids and oligonucleotides used in this study.

Strains	**Properties**	**Reference**
C. burnetii Nine Mile Phase II (NMII), RSA439	Plaque purified *C. burnetii* Nine Mile phase II (NMII), strain RSA439, clone 4 (wild type)	(24)
C. burnetii NMII pBlaM-MceA	Wild type carrying pBlaM-MceA (Cm^R)	(17)
C burnetii NMII pBlaM-Cig2	Wild type carrying pBlaM-Cig2 (Cm^R)	(16)
C. burnetii NMII P311-lux	Wild type carrying pTN7-Kan-311-*luxCDABE*-TT (Kan^R)	This study
C. burnetii NMII PicmW-lux	Wild type carrying pTN7-Kan-icmW-*luxCDABE*-TT (Kan^R)	This study
C. burnetii NMII Pcig2-lux	Wild type carrying pTN7-Kan-cig2-*luxCDABE*-TT (Kan^R)	This study
C. burnetii NMII *pmrA*::Tn	Transposon inserted at site 1177165 interrupting *pmrA* gene (Cm^R)	(16)
C. burnetii NMII *pmrA*::Tn P311-lux	*pmrA* transposon mutant carrying pTN7-Kan-311-*luxCDABE*-TT (Cm^R Kan^R)	This study
C. burnetii NMII *pmrA*::Tn PicmW-lux	*pmrA* transposon mutant carrying pTN7-Kan-icmW-*luxCDABE*-TT (Cm^R Kan^R)	This study
C. burnetii NMII *pmrA*::Tn Pcig2-lux	*pmrA* transposon mutant carrying pTN7-Kan-cig2-*luxCDABE*-TT) (Cm^R Kan^R)	This study
Escherichia coli DH5α	F- Φ80*lac*ZΔM15 Δ(*lac*ZYA-*arg*F) U169 *rec*A1 *end*A1 *hsd*R17 (rK-, mK+) *pho*A *sup*E44 λ- *thi*-1 *gyr*A96 *rel*A1	Invitrogen
E. coli PIR1	F- *Δlac169 rpoS(Am) robA1 creC510 hsdR514 endA recA1 uidA(ΔMluI)::pir-116*	Invitrogen
E. coli PIR2	F- *Δlac169 rpoS(Am) robA1 creC510 hsdR514 endA recA1 uidA(ΔMluI)::pir*	Invitrogen
Plasmids	**Properties**	**Reference**
pBlaM-MceA	*Coxiella* vector pJB-CAT-BlaM containing *mceA* (*cbu0077)* at the *Sal*I site to create a BlaM fusion construct under the control of CBU1169 promoter	(17)
pBlaM-Cig2	*Coxiella* vector pJB-CAT-BlaM containing *cig2* (*cbu0021*) at the *Sal*I site to create a BlaM fusion construct under the control of CBU1169 promoter	(16)
pSpCas9(BB)-2A-Puro	Addgene plasmid #62988	(25)

(pX459) V2.0		
pX459-LRP1-Exon-1	Contains guide RNA for LRP1 Exon 1 inserted into the *Bbs*I site of pX459	This study
pX459-M6PR-Exon-2	Contains guide RNA for M6PR Exon 2 inserted into the *Bbs*I site of pX459	This study
pX459-M6PR-Exon-3	Contains guide RNA for M6PR Exon 3 inserted into the *Bbs*I site of pX459	This study
pX459-TPP1-Exon-2	Contains guide RNA for TPP1 Exon 2 inserted into the *Bbs*I site of pX459	This study
pX459-TPP1-Exon-3	Contains guide RNA for TPP1 Exon 3 inserted into the *Bbs*I site of pX459	This study
pMiniTN7T-Kan		P. Beare
pMiniTn7T-CAT::*luxCDABE*		(9)
pTN7-Kan-*luxCDABE*-TT	Promoterless *luxCDABE* fragment cloned into pMiniTN7T-Kan via *Kpn*I-*Nhe*I digest, with T0T1 terminator added via *Kpn*I digest	This study
pTN7-Kan-311-*luxCDABE*-TT	*cbu0311* promoter cloned into pTN7-Kan-*luxCDABE*-TT	This study
pTN7-Kan-icmW-*luxCDABE*-TT	*icmW* promoter cloned into pTN7-Kan-*luxCDABE*-TT	This study
pTN7-Kan-cig2-*luxCDABE*-TT	*cig2* promoter cloned into pTN7-Kan-*luxCDABE*-TT	This study
pTNS2::*P1169-tnsABCD*		(26)
Oligonucleotide	**Sequence**	**Use/Reference**
OmpA-F	CAGAGCCGGGAGTCAAGCT	Quantification of Coxiella genomes in qPCR
OmpA-R	CTGAGTAGGAGATTTGAATCGC	Quantification of Coxiella genomes in qPCR
18S-F	CGGCTACCACATCCAAGGAA	RT-qPCR
18S-R	GCTGGAATTACCGCGGCT	RT-qPCR
Rab7A-F	AGGAAGAAAGTGTTGCTGAAGG	RT-qPCR
Rab7A-R	TGATGTCTTCCCGACTCCA	RT-qPCR
LRP1-F	CTGCTCTCAGCTCTGGTCG	RT-qPCR
LRP1-R	CCAGCCCTTTGAGATACAGG	RT-qPCR
M6PR-F	TGGCTACTCCAGTTTCCCAC	RT-qPCR

M6PR-R	ATTCTCTCACTGCCACAGCC	RT-qPCR
LRP1-F (Exon 1)	CACCGGCAACGGCGGGGTCAGCA	CRISPR guide (27)
LRP1-R (Exon 1)	AAACTGCTGACCCCGCCGTTGCC	CRISPR guide (27)
M6PR-F (Exon 2)	CACCGGAAAAAACTTGCGACTTGGT	CRISPR guide
M6PR-R (Exon 2)	AAACACCAAGTCGCAAGTTTTTTCC	CRISPR guide
M6PR-F (Exon 3)	CACCGGAAGCTGGCAACCACACTTC	CRISPR guide
M6PR-R (Exon 3)	AAACGAAGTGTGGTTGCCAGCTTCC	CRISPR guide
TPP1-F (Exon 2)	CACCGGTCCTCCGCTGGTCGGGCTC	CRISPR guide
TPP1-R (Exon 2)	AAACGAGCCCGACCAGCGGAGGACC	CRISPR guide
TPP1-F (Exon 3)	CACCGGTGTGGAAAGACTCTCGGAGC	CRISPR guide
TPP1-R (Exon 3)	AAACGCTCCGAGAGTCTTTCCACACC	CRISPR guide
CBU0311 promoter-F	GTCGACGGTATCGATAAGCTAGCGGATCCCAG TCTGATTATTAATTCAAACGGGTCAGGA	Luciferase reporters
CBU0311 promoter-R	AATAATGAATGAAATTTTTTTAGTCATATTTGCC ATAAGGGCCCTCCTTCATGAGCGCAA	Luciferase reporters
Cig2 promoter-F	GTCGACGGTATCGATAAGCTAGCGGATCCCAG TCTCCTCATTTACAACAAACTTCT	Luciferase reporters
Cig2 promoter-R	CCGTTAATAATGAATGAAATTTTTTTAGTCATAT TTGCCATGTTTATCTCCAGCGCTT	Luciferase reporters
IcmW promoter-F	GTCGACGGTATCGATAAGCTAGCGGATCCCAG TCTCATTCATGCTAGCACCACTTCC	Luciferase reporters
IcmW promoter-R	GTTAATAATGAATGAAATTTTTTTAGTCATATTT GCCATGACTTCTCCGCTATTTAGGGT	Luciferase reporters
T0T1-F	TAGGTACCCTTGGACTCCTGTTGATAGATCCAG TAATGAC	Luciferase reporters
T0T1-R	ACGGTACCCTCCTAGCGGCGGATTTGTCCTAC	Luciferase reporters

Dataset S1: Summary of the siRNA primary screen outcome.

Dataset S2: Summary of the validation screen outcome of the 400 genes selected.

Dataset S3: Classification of the genes within the validation screen. Targets were sorted into three categories: high-confidence validation (4/4 – green or 3/4 – blue), moderate-confidence validation (2/4 – yellow) and did not validate (1/4 or 0/4 – white).

Dataset S4-6: RNA-seq raw data, including the $\log_2$ fold change and padj values used to generate heat maps (Figure 4) for the 62 genes common to both Beare *et al* (9) and this study: WT H_20 vs *pmrA*::Tn H_20 (Dataset S4); WT AA vs WT H_20 (Dataset S5); *pmrA*::Tn AA vs *pmrA*::Tn H_20 (Dataset S6). (AA – Amino acids).

References:

1. A. Birmingham *et al.*, Statistical methods for analysis of high-throughput RNA interference screens. *Nat Methods* **6**, 569-575 (2009).
2. P. D. Thomas *et al.*, PANTHER: a browsable database of gene products organized by biological function, using curated protein family and subfamily classification. *Nucleic Acids Res* **31**, 334-341 (2003).
3. E. A. Latomanski, P. Newton, C. A. Khoo, H. J. Newton, The Effector Cig57 Hijacks FCHO-Mediated Vesicular Trafficking to Facilitate Intracellular Replication of *Coxiella burnetii*. *PLoS Pathog* **12**, e1006101 (2016).
4. E. Martinez, F. Cantet, M. Bonazzi, Generation and multi-phenotypic high-content screening of Coxiella burnetii transposon mutants. *J Vis Exp*, e52851 (2015).
5. K. Jaton, O. Peter, D. Raoult, J. D. Tissot, G. Greub, Development of a high throughput PCR to detect *Coxiella burnetii* and its application in a diagnostic laboratory over a 7-year period. *New Microbes New Infect* **1**, 6-12 (2013).
6. P. Newton, E. A. Latomanski, H. J. Newton, Applying Fluorescence Resonance Energy Transfer (FRET) to Examine Effector Translocation Efficiency by *Coxiella burnetii* during siRNA Silencing. *J Vis Exp* (2016).
7. N. L. Bray, H. Pimentel, P. Melsted, L. Pachter, Near-optimal probabilistic RNA-seq quantification. *Nat Biotechnol* **34**, 525-527 (2016).
8. S. Anders, W. Huber, Differential expression analysis for sequence count data. *Genome Biol* **11**, R106 (2010).
9. P. A. Beare *et al.*, Essential Role for the Response Regulator PmrA in *Coxiella burnetii* Type 4B Secretion and Colonization of Mammalian Host Cells. *J Bacteriol* **196**, 1925-1940 (2014).
10. J. C. Oliveros (2007-2015) Venny. An interactive tool for comparing lists with Venn's Diagrams.
11. A. I. Saeed *et al.*, TM4 microarray software suite. *Methods Enzymol* **411**, 134-193 (2006).
12. M. Thelen, D. Winter, T. Braulke, V. Gieselmann, SILAC-Based Comparative Proteomic Analysis of Lysosomes from Mammalian Cells Using LC-MS/MS. *Methods Mol Biol* **1594**, 1-18 (2017).
13. Z. Lifshitz *et al.*, Identification of novel *Coxiella burnetii* Icm/Dot effectors and genetic analysis of their involvement in modulating a mitogen-activated protein kinase pathway. *Infect Immun* **82**, 3740-3752 (2014).
14. C. L. Larson *et al.*, *Coxiella burnetii* effector proteins that localize to the parasitophorous vacuole membrane promote intracellular replication. *Infect Immun* (2014).
15. Z. Lifshitz *et al.*, Computational modeling and experimental validation of the *Legionella* and *Coxiella* virulence-related type-IVB secretion signal. *Proc Natl Acad Sci U S A* **110**, E707-715 (2013).
16. H. J. Newton *et al.*, A screen of *Coxiella burnetii* mutants reveals important roles for Dot/Icm effectors and host autophagy in vacuole biogenesis. *PLoS Pathog* **10**, e1004286 (2014).

17. K. L. Carey, H. J. Newton, A. Luhrmann, C. R. Roy, The *Coxiella burnetii* Dot/Icm system delivers a unique repertoire of type IV effectors into host cells and is required for intracellular replication. *PLoS Pathog* **7**, e1002056 (2011).
18. L. F. Fielden *et al.*, A Farnesylated *Coxiella burnetii* Effector Forms a Multimeric Complex at the Mitochondrial Outer Membrane during Infection. *Infect Immun* **85** (2017).
19. C. Chen *et al.*, Large-scale identification and translocation of type IV secretion substrates by *Coxiella burnetii*. *Proc Natl Acad Sci U S A* **107**, 21755-21760 (2010).
20. M. M. Weber *et al.*, Identification of *Coxiella burnetii* type IV secretion substrates required for intracellular replication and Coxiella-containing vacuole formation. *J Bacteriol* **195**, 3914-3924 (2013).
21. C. L. Larson, P. A. Beare, D. Howe, R. A. Heinzen, *Coxiella burnetii* effector protein subverts clathrin-mediated vesicular trafficking for pathogen vacuole biogenesis. *Proc Natl Acad Sci U S A* **110**, E4770-4779 (2013).
22. D. E. Voth *et al.*, The *Coxiella burnetii* ankyrin repeat domain-containing protein family is heterogeneous, with C-terminal truncations that influence Dot/Icm-mediated secretion. *J Bacteriol* **191**, 4232-4242 (2009).
23. D. E. Voth *et al.*, The *Coxiella burnetii* cryptic plasmid is enriched in genes encoding type IV secretion system substrates. *J Bacteriol* **193**, 1493-1503 (2011).
24. P. A. Beare *et al.*, Comparative genomics reveal extensive transposon-mediated genomic plasticity and diversity among potential effector proteins within the genus *Coxiella*. *Infect Immun* **77**, 642-656 (2009).
25. F. A. Ran *et al.*, Genome engineering using the CRISPR-Cas9 system. *Nat Protoc* **8**, 2281-2308 (2013).
26. P. A. Beare, C. L. Larson, S. D. Gilk, R. A. Heinzen, Two systems for targeted gene deletion in *Coxiella burnetii*. *Appl Environ Microbiol* **78**, 4580-4589 (2012).
27. L. Luo *et al.*, TLR Crosstalk Activates LRP1 to Recruit Rab8a and PI3Kgamma for Suppression of Inflammatory Responses. *Cell Rep* **24**, 3033-3044 (2018).